Available online at www.sciencedirect.com
ScienceDirect
Journal of the European Ceramic Society 31 (2011) 3–11
www.elsevier.com/locate/jeurceramsoc

Influence of particles packing in granules on the particles orientation in compacts

M. Imran Zainuddin [a,b,*], S. Tanaka [a], R. Furushima [a], K. Uematsu [a]

[a] Department of Chemistry, Nagaoka University of Technology, 1603-1 Kamitomioka, Nagaoka, Niigata 940-2188, Japan
[b] Faculty of Chemical Engineering, University Teknologi MARA, 40450 Shah Alam, Selangor, Malaysia

Received 5 February 2010; received in revised form 1 September 2010; accepted 9 September 2010

Abstract

Particles orientation during compaction was studied in alumina granules of different packing structures and deformation properties. These granules were classified mainly in two types: loose granules prepared with flocculated slurries and dense granules prepared with dispersed slurries. Particles orientations in the granules and in the compacts were examined quantitatively with the cross-polarized light microscopy. A large difference was noted in the packing structures of granules and compacts. Orientation of particles was detected only in the surface vicinity of the dense granules. These dense granules show only a slight change in particle orientation locally and its initial structures were mostly preserved even after compaction. As a result, the green compacts containing these granules also show very low net particles orientation. In contrast, loose granules show no orientated particles. However, a major rearrangement of the particles was noted during compaction, resulting in a high net particle orientation in the compacts. The particles orientation in the green compacts affected the anisotropy in the sintering shrinkage significantly; high anisotropy was observed in compacts of high particle orientation fabricated from the loose granules.

Keywords: Pressing; Microstructure – prefiring; Microstructure – final; Optical microscopy; Mechanical properties

1. Introduction

Particle orientation often occurs in powder compact made from commercial alumina powder, causing anisotropic shrinkage during sintering which leads to deformation or warping of the final product.[1–4] The development of particle orientation has been explained as follows; due to the elongated shape of the commercial alumina particles, the applied stress during compaction rearranges the particles with their longest shape axis normal to the direction of pressing. Furthermore, the resultant compact may also shows non-uniform packing density where loose and tight packing exists in the directions perpendicular and parallel to the direction of pressing, respectively. The suppression of particle orientation is the key for minimizing the deformation in sintering. Clearly, it is necessary to understand the factors that affect the particle orientation.

The packing structure of particles in the granules should play an important role in developing the particle orientation, since it governs the deformation property of the granules and thus the rearrangement of particles during compaction. Particles in the loosely packed granules should be more mobile than in the densely packed granules, that is, particles in the former granules should be more liable to orientation during compaction, thus causing anisotropic shrinkage during sintering. Two types of alumina granules were considered in the study; (1) granules of loosely packed particles prepared from flocculated slurry, and (2) granules of densely packed particles prepared from dispersed slurry (hereafter, they will be referred as the loose granules and the dense granules, respectively).

The objective of this study is to determine the relationship among the granules properties, particle orientation in the green compacts and their sintering behavior. The granule properties considered in this study are packing structure, density and

* Corresponding author at: Department of Chemistry, Nagaoka University of Technology, 1603-1 Kamitomioka, Nagaoka, Niigata, Japan.
Tel.: +81 258 47 4317; fax: +81 258 47 9337.
E-mail addresses: zainuddin_mohd_imran@mst.nagaokaut.ac.jp, eemran04@yahoo.com (M.I. Zainuddin).

0955-2219/$ – see front matter © 2010 Elsevier Ltd. All rights reserved.
doi:10.1016/j.jeurceramsoc.2010.09.011

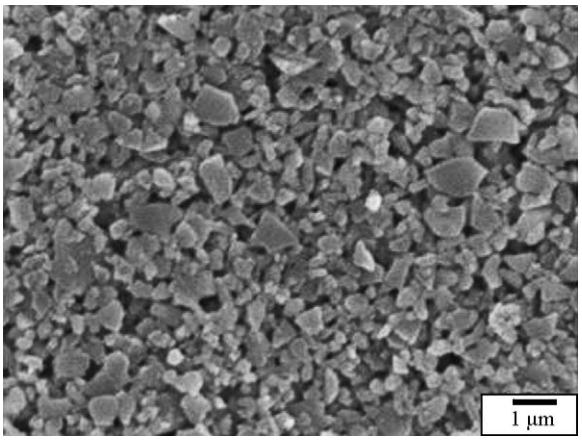

Fig. 1. SEM micrograph of alumina particles.

deformation behavior. The cross-polarized light microscopy[5,6] was used to characterize the particles packing structures within granules as well as in compacts. The sintering shrinkages of die pressed compacts were measured for the directions of thickness and diameter at intermediate and final stages of sintering to discuss the relevance between the structure and the anisotropic shrinkage.

2. Experimental

A commercial alumina powder (AL160-SG3, average particle size 0.6 μm, 99.8% of purity, Showadenko, Japan) was used as a raw material (Fig. 1). Particles of this powder have elongated shapes, which is a normal characteristic for this type of industrial grade powder. Four kinds of aqueous slurries were formulated in preparing two types of granules of different particle packing; loose and dense packed granules, with two different kinds of solid content each. Ammonium polyacrylate-base solution (SERUNA D-305, Chukyoyushi, Japan) was used as dispersant in the range of 0–1.0 wt%. Polyvynil alcohol (PVA) binder (PVA105, Kurarays, Japan) was added at the amount of 0.5 wt% in all slurries to enhance the granules strength for handling purposes. All additives contents are based on the dry weight of alumina powders. The slurries compositions in detail are shown in Table 2. Attrition milling (SC mill, Mitsui Mining, Japan) using zirconia beads ($\phi = 300$ μm) as milling media was applied for mixing. The slurry was spray-dried into granules with a spray-dryer of inner diameter 1.3 m (SD13, Mitsui Mining, Japan) at the inlet and outlet air temperature of 200 °C and 100 °C, respectively. During dry-pressing, granules were pressed uniaxially in a die at 20 MPa followed by cold isostatic pressing (CIP) at 200 MPa. Pressed compacts were sintered at 1300, 1500 and 1600 °C for 1 h (10 °C/min). Porosities of the granules and green compacts were measured by a mercury intrusion porosimeter (Micromeritics, Pore Sizer 9320, Shimadzu, Japan). The deformation behavior of a single granule was examined by a micro-compression-testing machine (MCTE-500, Shimadzu, Japan) at the loading rate of 0.089 mN/s. The examinations were conducted under constant temperature of 25 °C, and relative humidity of 50%. A total of 20 granules of diameter between 50 and 70 μm were measured one by one for each type of granules. The internal microstructures of respective green compacts were examined by the IR microscopy.[7] The powder tester (PT-R, Hosokawa Micron, Japan) was used to determine the packing fraction in the die by filling the granules in a container of 100 ml. The packing fractions were measured at as-filled and after tapping for 180 times. Packing structure of particles was examined for granules, green compacts and compacts sintered at 1300 °C by the liquid immersion technique with a crossed polarized light microscope (OPTIPHOT2-POL X2TP, Nikon, Japan) under transmission mode. Methylene iodide solution was used as the immersion liquid where sulfur (99.5% of purity, 33% of saturation) was added into the immersion liquid to achieve almost equal refractive index as to alumina. Samples sintered at 1300 °C and green compacts were cut and ground with abrasive paper (grid #800) to make a thin specimen (350 ± 30 μm) for examination using the liquid immersion technique. The thickness of specimens was determined by micrometer. The samples were examined in the normal direction to the uniaxial pressing. The micrographs were taken at two angles of rotation separated by 45°. The particle orientation in the compacts was quantitatively determined with a Berek compensator (Nichika, Japan).[8–10] The density of compacts was determined by Archimedes method prior to cutting. The anisotropy in the sintering shrinkage was represented by the shrinkage ratio defined as shrinkage in the axial direction over shrinkage in the diametric direction.

3. Results

Fig. 2 shows the scanning electron micrographs of the alumina granules. The morphologies of the granules made from flocculated and dispersed slurries are spherical and dimpled, respectively. The granules were denominated as L1 and L2 for loose granules, and D1 and D2 for dense granules. The respective densities were 43.0 and 50.2% for the former, and 54.0 and 56.9% for the latter, respectively. The properties of slurries and the resultant granules are summarized in Table 1. A strong correlation between the properties of slurry and granules is shown.

Fig. 3 shows the cross-polarized light micrographs of granules showing internal particles packing structure. Under the cross-polarized light microscope, dark to bright images are observed according to the angle of particles crystallographic axis; namely *c*-axis at which the polarized light propagates through. Dark images are produced when polarized light propagates parallel to the *c*-axis of the particles, while, dim to bright images are produced when the polarized light propagates off the *c*-axis, where the brightness are dependent of the light propagation angle to the *c*-axis of the particles.[11,12] For alumina particles, the shortest and the longest particles shape axis correspond to the *c* and *a* crystallographic axis of the alumina particles, respectively. Furthermore, the *c*-axis is identical to the optical axis for alumina hexagonal crystal. Therefore, the particles orientation can be easily recognized under the cross-polarized light microscopes. From the figure, the loose granules L1 and L2 show a dark matrix with scattered bright features of about 2–5 μm

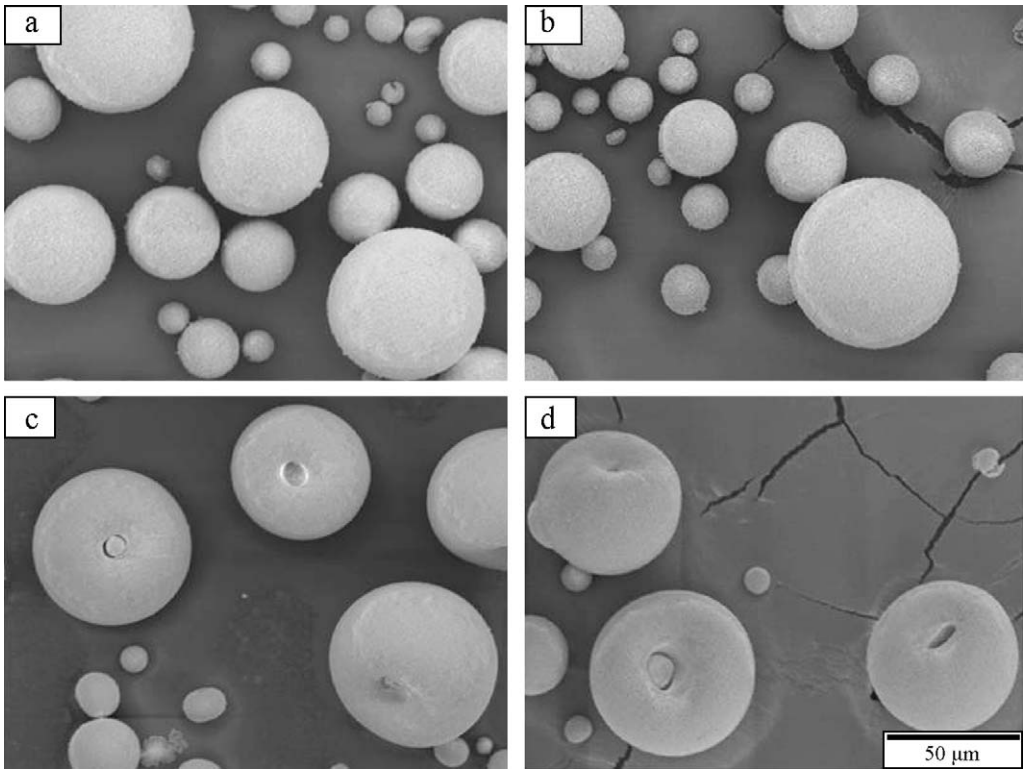

Fig. 2. SEM micrograph of granules morphology prepared from respective slurries. (a) L1, (b) L2, (c) D1 and (d) D2.

in size. These bright features correspond to coarse particles or agglomerates, which survived the milling process. In contrast, the dense granules D1 and D2 show a pattern of bright zones in form of quadrants centered at the dimples. The dark sites indicate that the particles *c*-axis is normal to the granules diametric direction, thus making the *a*-axis i.e., the longest shape axis of the alumina particles is parallel to the granules surface. Furthermore, the pattern of the quadrant does not change when the granules are rotated on its axis which suggests an identical structure of particles at the granules surface.

Fig. 4 shows the representative deformation behavior for individual granules under compression. For all type of granules, stress increases linearly at low strain and then increases gradually and eventually come to a plateau as strain increases. Here, the increasing of strain without accompanied by increasing stress indicates the fracture of granules, and the gradual increment indicates the yielding of granules. The intersection of extrapolation of the linear gradient and the plateau was used to determine the fracture stress, σ_f and the starting point of the curvature to determine the yield stress, σ_y of the granule as shown for granule D2, as an example, in Fig. 4. Similar method was applied in determining yield and fracture stress of the other types of granules and their values are summarized in Table 2. Loose granules L1 and L2 show almost similar low yield and fracture stresses, whereas the dense granules D1 and D2 show higher yield and fracture stresses. Notice that granules of similar shape but higher solid content show lower fracture strain which indicate their brittle fracture behavior. It is also interesting that despite of higher solid content and granule density of granule L2, it is only as hard as L1.

Fig. 5 shows the internal microstructure of respective green compacts examined by the liquid immersion infrared microscopy. Traces of granules boundaries (marked by white arrows) are observed in all specimens and more significant for D1 and D2 compacts. Dark areas (marked by black arrows) are observed in the center of granules in L1 and L2 compacts which indicate low density areas resulted from low particle packing within the granules itself. On the other hand, D1 and D2 show traces of collapsed dimple (marked by white dashed arrows) in the granules center.

Table 1
Properties of granules prepared from respective slurries.

Slurry			Granule			
Type	Solid content [vol.%]	Dispersant content [wt%]	Type	Denomination	Morphology	Density [%]
Flocculated	20	0	Loose	L1	Spherical	43.0
	30	0.3		L2	Spherical	50.2
Dispersed	30	1.0	Dense	D1	Dimpled	54.0
	40	1.0		D2	Dimpled	56.9

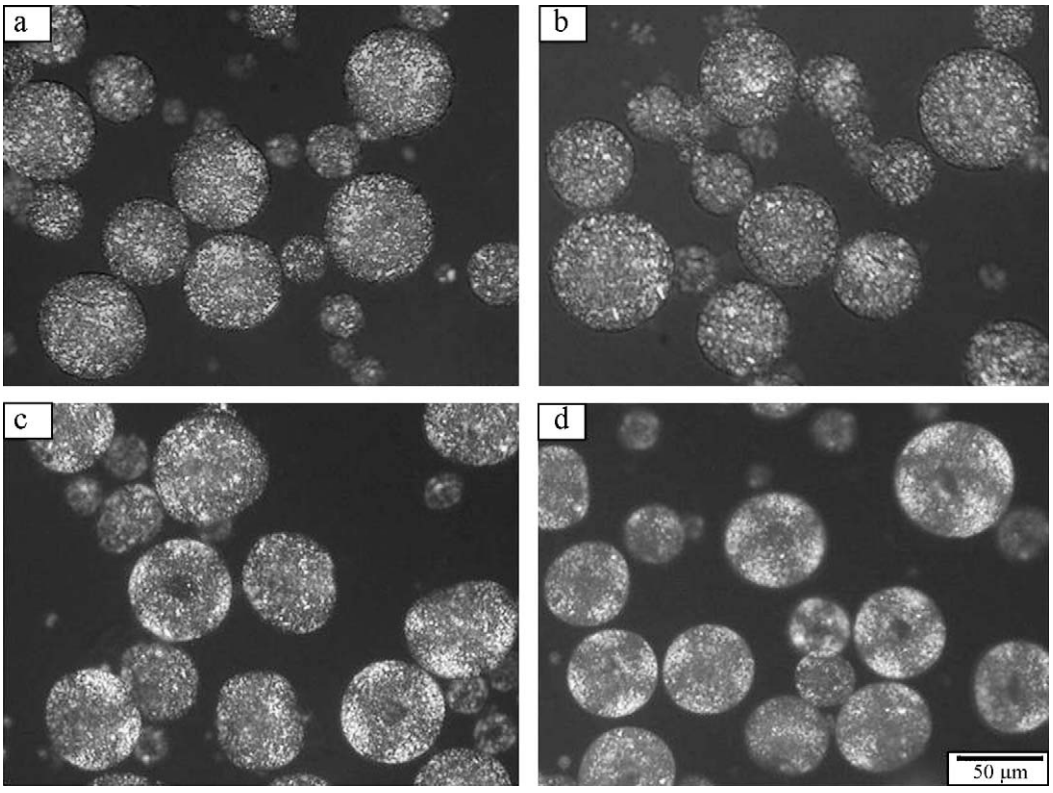

Fig. 3. Cross-polarized micrograph of granules showing internal particles packing structure. (a) L1, (b) L2, (c) D1 and (d) D2.

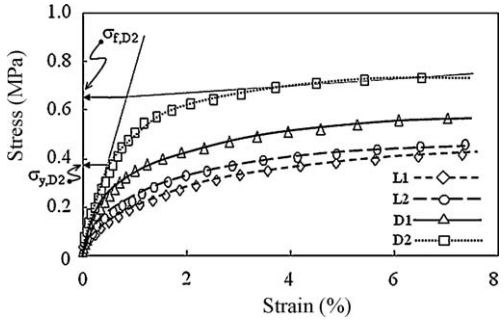

Fig. 4. Stress–strain diagram of single granule compaction showing representative deformation behavior for individual granules under compression.

Fig. 6 shows the variation of packing fraction with the compaction stress for respective granules. The loose granules show lower packing fraction than the dense granules throughout the compaction process. The packing fraction due to tapping shows higher value with increasing granules density. D2 shows the highest packing fraction throughout the overall compaction processes followed by D1, L2 and L1. During uniaxial pressing, the dense and the loose granules show different compaction behaviors. For dense granules D1 and D2, two points of gradient transition were observed along the curve. Here, points of gradient transition were determined using the extrapolation method where the first point of gradient transition is also known as yield stress which indicates granules strength. These points occur at 0.23 and 3.30 MPa for D1, and 0.25 and 2.15 MPa for D2. In contrast, only one point of gradient transition was observed for loose granules L1 and L2 which occur at 0.17 and 0.19 MPa, respectively. This difference in numbers of point of gradient transition can be related to the variation of densification mechanism of both loose and dense granules during compaction. Subsequent cold isostatic pressing (CIP) of uniaxially pressed compacts increases the packing fractions for all specimens. The relative green densities of compacts were 57.0, 57.2, 57.9 and 58.5% for L1, L2, D1 and D2, respectively. It is important to note that almost the same packing fraction was attained for both types of granules. During

Table 2
Stress and strain of yield and fracture point of single granule compaction test.

Type of granule	Yield point		Fracture point	
	Stress, σ_y (MPa)	Strain ε_y (%)	Stress, σ_f (MPa)	Strain ε_f (%)
L1	0.15	1.3	0.33	7.6
L2	0.17	1.5	0.35	6.0
D5	0.25	1.3	0.56	15.2
D2	0.31	1.1	0.66	11.2

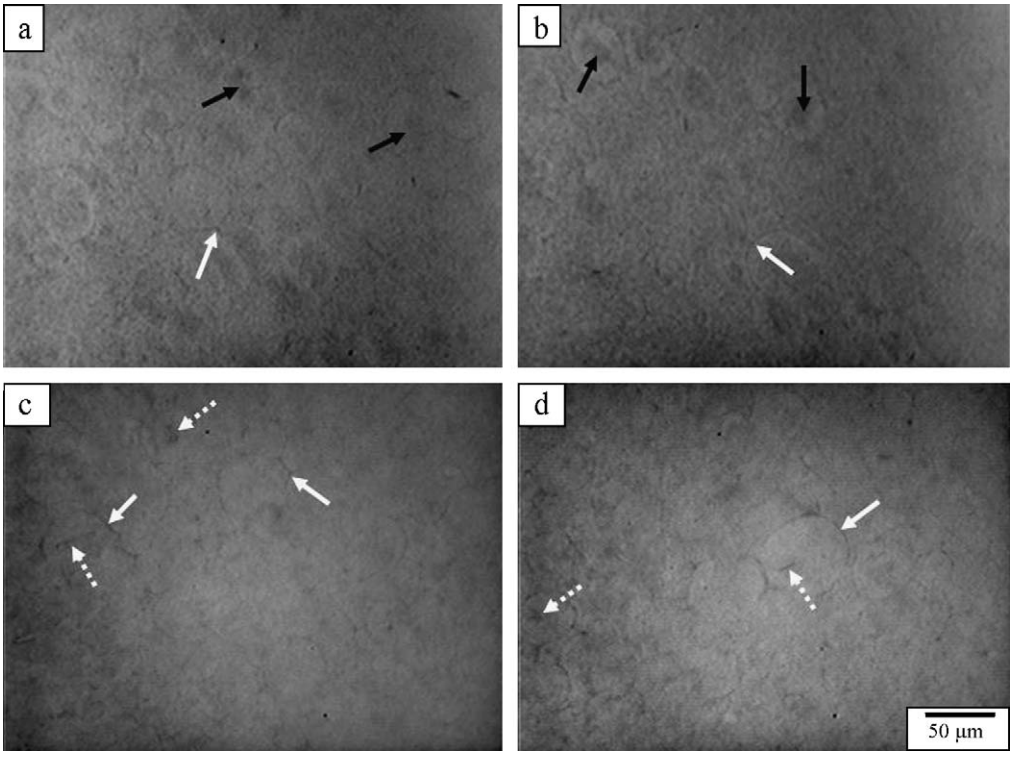

Fig. 5. Micrographs of internal microstructures of respective green compacts examined by the liquid immersion infrared microscopy. (a) L1, (b) L2, (c) D1 and (d) D2.

CIP, it is shown that the packing fraction increases more significantly for the loose granules compared to the dense granules. This suggests that the particle rearrangement should be much more drastic in the loose granules.

Fig. 7 shows the packing structures of particles in respective green compacts examined by the cross-polarized light microscopy. The top and bottom micrographs are of the same specimens which are separated by rotation of 45° during examination. Bright and dark regions in the micrographs indicate that the optical property, which corresponds to the packing structure of particles, is locally different in the compact. In the region where bright to dark changes with rotation is observed, the alumina particles of elongated shape must be oriented with their *c*-axis, i.e., the shortest side of the particle, parallel to the direction of pressing. A significant difference is noted in the optical image for the compacts fabricated with the loose and the dense granules. In the compact fabricated with the loose granules, the bright region appears layer-like over the whole sample at a certain angle of rotation. This bright region disappears almost simultaneously by a 45° rotation. This confirms that the *c*-axis of alumina particles are oriented parallel to the direction of pressing. In contrast, dark and bright zones are always observed at 0° and 45° in the compact fabricated with the dense granules. Detailed observations show that the individual region changes its brightness with the rotation. It can be noted that these dark and bright zones correspond to the image of bright quadrants observed in the dense granules as shown in Fig. 3. This indicates that the packing structure of particles in the dense granule was preserved even after pressing.

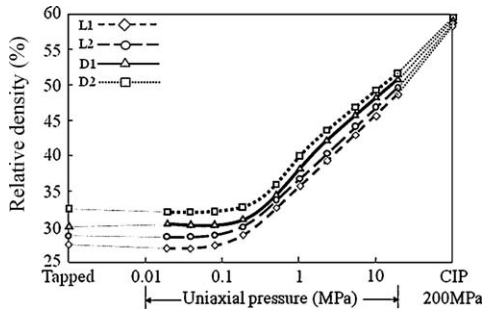

Fig. 6. Variation of packing fraction with the compaction steps for respective granules.

Fig. 8 shows the packing structure of particles in the respective compacts after sintering at 1300 °C. The packing structures were similar with those observed in the green compacts. Bright zones appear to be extended and more defined than those noted in the green compacts.

Table 3 lists the values of the orientation degree of the respective green compacts and compacts sintered at 1300 °C. The orientation degree is larger for compacts fabricated with loose granules than of those fabricated with dense granules. Similar tendency is observed after sintering at 1300 °C. There were no significant changes in degree of orientation before and after sintering.

Fig. 9 shows the relation between shrinkage ratio and sintering temperature of compacts fabricated with respective granules. Unity of the shrinkage ratio corresponds to the isotropic sintering shrinkage. The shrinkage ratios varied significantly with densification for the loose granules L1 and L2. In the intermediate

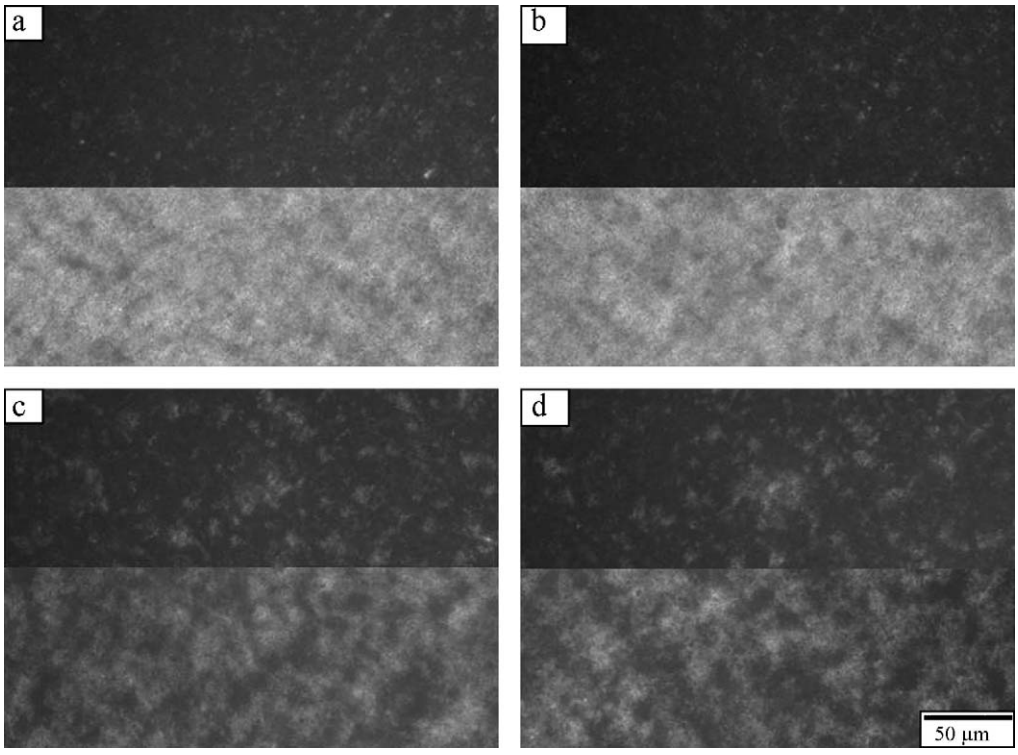

Fig. 7. Micrographs of packing structures of particles in respective green compacts examined by the cross-polarized light microscopy. (a) L1, (b) L2, (c) D1 and (d) D2. The upper and lower micrographs are separated by rotation of 45°.

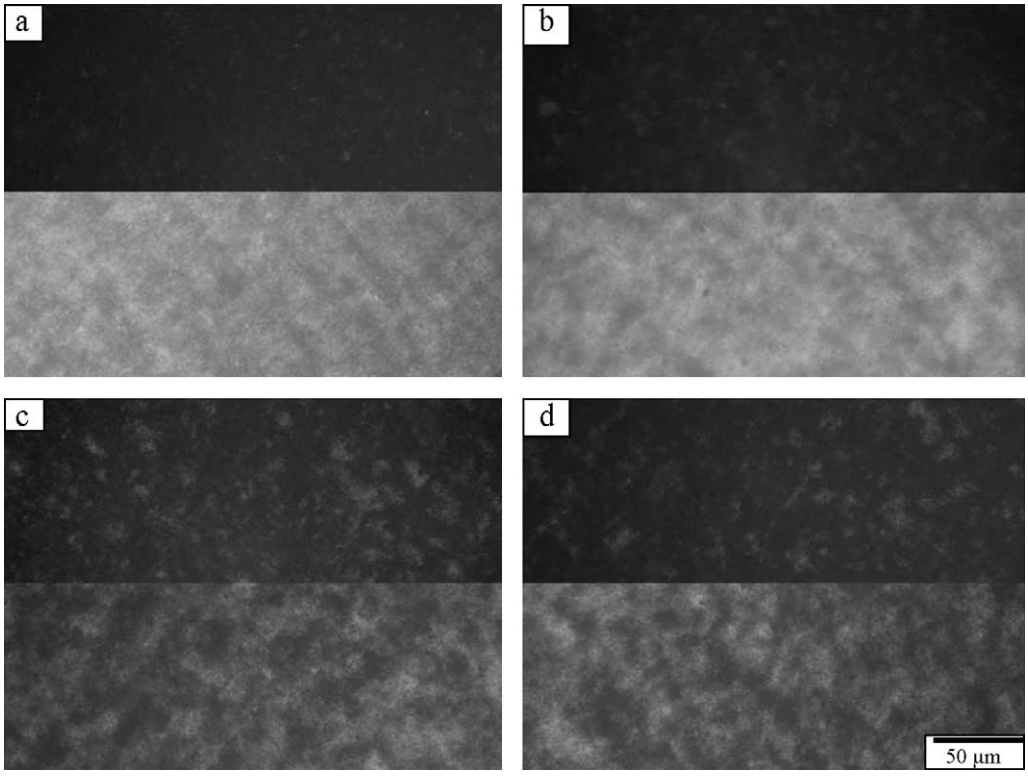

Fig. 8. Micrographs of packing structures of particles in respective compacts sintered at 1300 °C examined by the cross-polarized light microscopy. (a) L1, (b) L2, (c) D1 and (d) D2. The upper and lower micrographs are separated by rotation of 45°.

Table 3
Degree of particle orientation of green compacts and compacts sintered at 1300 °C.

Granule type	Orientation degree (%)	
	Green compact	Sintered at 1300 °C
L1	4.8 ± 0.1	4.5 ± 0.1
L2	5.7 ± 0.1	5.0 ± 0.1
D1	3.2 ± 0.1	4.0 ± 0.1
D2	3.4 ± 0.1	3.0 ± 0.1

stage of sintering (at 1300 °C), very large shrinkage ratios were noted. They decreased with increasing sintering temperature and came close to unity at 1600 °C. In contrast, shrinkage ratios were almost constant for the dense granules D1 and D2 with increasing sintering temperature. At the end of sintering (at 1600 °C), L1 shows the highest shrinkage ratio, while L2, D1 and D2 show almost isotropic shrinkage, especially for compacts fabricated with the dense granules D1 and D2.

4. Discussion

This study shows a clear relation between the structures of granules and compacts. Packing structure of particles in granules governs their orientation during pressing in the systems of commercial alumina powder of elongated shape. Loosely packed particles rearrange and orientate themselves easily during compaction; while densely packed particles are difficult to rearrange. The results are readily understandable based on the detailed packing structures shown above.

Particles acquire different packing structures during the formation of granules via spray drying of the slurry, forming granules of different morphologies; spherical (loose packing) and dimpled (dense packing) (Figs. 2 and 4). These differences in morphology and packing structure are clearly governed by the flocculation-dispersion of particles in the slurry, as shown in the Table 1. In this study, four types of granules were obtained from two different dispersion states of the slurries; flocculated and dispersed. Loose granules L1 and L2, consisted of low and mid solid content of 20 and 30 vol%, respectively. They were also formed with no and low dispersant content, respectively, which was insufficient to separate the particles within the slurry, thus

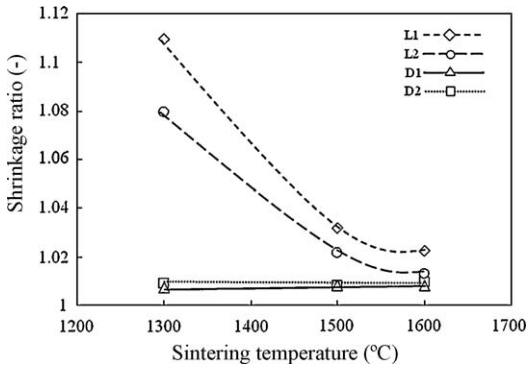

Fig. 9. Relation between shrinkage ratio and sintering temperature of compacts fabricated with respective granules.

the agglomeration of particles resulted in granules with loose packing structure. The dense granules D1 were formed from the slurry with mid solid content equal to L2 but with a dispersant content sufficient for a well-dispersed slurry. While, the dense granules D2 were formed from a well-dispersed slurry with the highest solid loading of 40 vol%, and shows the highest density. These results are in close agreement with findings in other publications.[13–15]

The cross-polarized micrographs (Fig. 3) explicitly show the difference in the packing structures of particles in the granules. Particles in the loose granules are randomly distributed due to agglomeration, i.e. their *c*-axes are randomly oriented in the granules as is revealed by the dark matrix of the micrographs. Orientation of particles is noted in the dense granules, resulting in the particular optical image of bright quadrants centered at the dimple. The longest shape axes of the particles are shown aligned to the surface of these granules. Similar observation was reported in our past publication.[5,16]

The packing structure of granules governs their deformation property (Fig. 4). Loose granules L1 and L2 showed lower strength compared to dense granules D1 and D2. Furthermore, dense granules D1 show higher granules strength compared to L2 although they were prepared from slurry of equal solid content. This clearly shows the particle packing structure within granules increases the strength of individual granule. Dimpled granules are harder due to dense particle arrangement and formation of thick shell of particles during drying.[17,18] Dense granules D2 show high resistance against deformation and have the highest strength. It is also interesting to note the difference in number of point of gradient transition between loose and dense granule. This can be related to the variation in densification mechanism of compacts due to the structure of the granules where dense granules contains dimple, while loose granules contains no dimple. In the case of dense granule with dimple i.e., D1 and D2, a significant increase in relative density of the compact is mainly due to the collapse of granules dimple. This occurs as compaction stress increases beyond the first point of gradient transition i.e., the yield stress. As compaction further increases, most of the granules dimple are collapsed and void between granules are decreased. Here after, further increase in relative density is assisted by particles rearrangement within the granules. Therefore, reduction in volume becomes less significant which leads to the second gradient transition of the relative densities curve. In contrast, for granules without dimple i.e., L1 and L2, the only point of gradient transition occurs when granules start to yield and/or break as compaction stress increases passes the yield point. Beyond the yield point, due to uniform distribution of internal pores within the granules, pores are expected to be reduced gradually and not abruptly such as for dense granules with dimple. Furthermore, particle rearrangement is also expected to occur simultaneously in assisting pores reduction. This is observed by the significant increases of particle orientation in compact containing granules without dimple compared to compact containing granules with dimple during uniaxial pressing.[19] In other words, the two stages of compact densification for dense granules with dimple i.e., granules deformation and particles rearrangement, are combined into one for loose

granules without dimple. Therefore, no high stress break for L1 and L2 were observed.

IR microscopy showed that the compact made with loose granules L1 and L2 have uniform structure with only slight traces of granules and pores. The traces of granules and pores are more significant in the dense granules D1 and D2 (Fig. 5). These formations of pores and granules traces are related to granules properties as has been discussed in past publications.[20,21] Here, surprisingly, despite of low strength of granules, low density areas within loose granules (L1 and L2) are difficult to be eliminated even after being CIPed at a very high pressure. This explains the relatively low green density compared to compacts made from dense granules.

It is very important to note that the compacts reached similar density after CIP, even though the starting granules are very different in density and microstructure. Clearly the rearrangement of particles during compaction is more drastic for the loose granules L1 and L2 compared to the dense granules D1 and D2. Particles in loosely packed granules must change their local position much more than those in tightly packed granules under pressure to reach the similar packing density after compaction.

Evolution of the internal microstructure should be closely related to the change of packing fraction. Loose and randomly packed particles oriented themselves during pressing, while densely packed particles remain almost unaltered. The particles are oriented in the compacts of loose granules L1 and L2 (Fig. 7). On the other hand, the particles in the dense granules D1 and D2 undergo less rearrangement due to their highly packed structure. Therefore, only low particles orientation was observed due to local orientation own by the granule structures remained in the green compact. This visual analysis was supported by the quantitative analysis for the orientation degree. Compacts fabricated with loose granules present higher orientation degree than those fabricated with dense granules.

The particles packing structure was similar before and after sintering at 1300 °C. Again, it is clearly that the particles are oriented in the compacts made from loose granules, while they are less oriented in compacts made from dense granules. The bright regions appear more defined after sintering, due to the initiation of the neck formation between particles. The values of orientation degree also show similar tendency as in the green compact; compacts made with loose granules show higher orientation degree than those made with dense granules.

The relation between packing structures of granules and the sintering behavior was also clearly defined. The compacts fabricated with the loose granules show higher particle orientation, and more significant anisotropic sintering shrinkage than those fabricated with dense granules. The anisotropic shrinkage associated to the particles orientation can be explained as follows. For compacts containing oriented particles in the axial direction, larger number of contacts per unit length exists in the same direction.[22] Initially, rapid sintering shrinkage occurs in this direction. Here, the elongated shape of particles contributes to the anisotropic grain growth, due to their anisotropy of surface energies.[23–25] In the intermediate stage, the development of long necks between particles slows down the sintering shrinkage in the axial direction relative to the lateral direction.[26] The result is the minimizing of the shrinkage anisotropy in the final stage of the sintering process. In this study, even though an isotropic shrinkage was finally obtained, it is most important to consider the change of sintering behavior; the change from anisotropic to isotropic shrinkage should involved the formation of voids and defects in the internal structure of compacts fabricated with loose granules.

5. Conclusions

The packing structure of particles in granules governs the orientation of particles in their respective compacts. Granules with loose packing structure of particles are easy to deform and the particles are liable to orientate during compaction. In contrast, granules with dense particle packing structure resists deformation and its structures remain even after compaction. The sintering shrinkage was found directly affected by the packing structure of particles in the granules. Significant anisotropy sintering shrinkage was observed in the compact of loose granules, in which higher particle orientation was detected. In the final stage of sintering, the shrinkage became more isotropic for all types of granules. The changes of the sintering behavior from anisotropic to isotropic shrinkage in compacts fabricated with loose granules were revealed.

Acknowledgement

This study is supported by The Program for Developing the Supporting System for Global Multidisciplinary Engineering Establishment under The Japanese Ministry of Education, Culture, Sports, Science and Technology.

References

1. Shui A, Zhang Y, Uchida N, Uematsu K. Origin of shape deformation during sintering of alumina compacts. *J Ceram Soc Japan* 1998;**106**:873–6 [in Japanese].
2. Shui A, Kato Z, Tanaka S, Uchida N, Uematsu K. Isotropic sintering shrinkage in pressed compact of near-spherical alumina particles. *Am Ceram Soc Bull* 2001;**80**:29–32.
3. Shui A, Kato Z, Tanaka S, Uchida N, Uematsu K. Sintering deformation caused by particle orientation in uniaxially and isostatically pressed alumina compacts. *J Eur Ceram Soc* 2002;**22**:311–6.
4. Shui A, Saito M, Uchida N, Uematsu K. Development of anisotropic microstructure in uniaxially pressed alumina compacts. *J Eur Ceram Soc* 2002;**22**:1217–23.
5. Uematsu K, Tanaka H, Zhang Y, Uchida N. Liquid immersion-polarized light microscopy as a powerful tool in the research of ceramic processing. *J Ceram Soc Japan* 1993;**101**(12):1400–3 [in Japanese].
6. Uematsu K, Ito H, Zhang Y, Uchida N. Novel characterization method for the processing of ceramics by polarized light microscope with liquid immersion technique. *Ceram Trans* 1995;**54**:83–9.
7. Uematsu K, Saito M. Liquid immersion technique coupled with infrared microscopy for direct observation of internal structure of ceramic powder compact, with alumina as an example. *J Mater Res* 1999;**14**(12):4463–5.
8. Shoji D. Microstructures and characteristics of ceramics with orientated grain in high magnetic field, Master thesis, Nagaoka University of Technology, Nagaoka, Niigata; 2000.
9. Makiya A. Production and evaluation of grain oriented ceramics in high magnetic field, Master thesis, Nagaoka University of Technology, Nagaoka, Niigata; 2001.

10. Makiya A, Tanaka S, Shoji D, Ishikawa T, Uchida N, Uematsu K. A quantitative evaluation method for particle orientation structure in alumina powder compacts. *J Eur Ceram Soc* 2007;**27**:3399–406.
11. Chantaramee N, Tanaka S, Kato K, Uchida N, Uematsu K. Characterization of particles packing in alumina green tape. *J Eur Ceram Soc* 2009;**29**:943–8.
12. Robinson PC, Savile B. *Qualitative polarized-light microscopy*. Oxford University Press and Royal Microscopical Society; 1992. pp. 10–14.
13. Lee H-W, Song H, Suk I-S, Oh S-R, Choi S-G. Effects of suspension property on granulate morphology and compaction behavior. *Ceram Trans J* 1995;**54**:41–5.
14. Tsubaki J, Hirose T, Shiota K, Utsumi R, Mori H. Dependence of slurry characteristics on shape forming process of spray-dried granules. *J Ceram Soc Japan* 1998;**106**(12):1210–4 [in Japanese].
15. Walker WJ, Reed JS, Verma SK. Influence of slurry parameters on the characteristics of spray-dried granules. *J Am Ceram Soc* 1999;**82**(7):1711–9.
16. Uematsu K, Ohsaka S, Shinohara N, Okumiya M. Grain-oriented microstructure of alumina ceramics made through the injection molding process. *J Am Ceram Soc* 1997;**80**(5):1313–5.
17. Tanaka S, Pin CC, Uematsu K. Effect of organic binder segregation on sintered strength of dry-pressed alumina. *J Am Ceram Soc* 2006;**89**(6):1903–7.
18. Zainuddin MI, Tanaka S, Uematsu K. The effect of segregation of polyacrylic acid (PAA) binder on green strength of dry-pressed alumina compacts. *J Am Ceram Soc* 2008;**91**(12):3896–902.
19. Zainuddin MI, Tanaka S, Uematsu K. Effect of polyacrylic acid (PAA) binder system on particle orientation during dry-pressing. *Powder Technol* 2009;**196**:133–8.
20. Zhang Y, Uchida N, Uematsu K. Direct observation of non-uniform distribution of PVA binder in alumina green body. *J Mater Sci* 1995;**30**:1357–60.
21. Takahashi H, Shinohara N, Uematsu K, Tsubaki J. Influence of granule character and compaction on the mechanical properties of sintered silicon nitride. *J Am Ceram Soc* 1996;**79**(4):843–8.
22. Coble RL. Sintering crystalline solids II experimental test of diffusion models in powder compacts. *J Appl Phys* 1961;**32**(5):793–9.
23. Seabaugh MM, Kerscht IH, Messing GL. Texture development by template grain growth in liquid-phase-sintered alpha-alumina. *J Am Ceram Soc* 1997;**80**(5):1181–8.
24. Kunaver U, Kolar D. Computer simulation of anisotropic grain growth in ceramics. *Acta Metall Mater* 1993;**41**(8):255–63.
25. Yang W, Chen LQ, Messing GL. Computer simulation of anisotropic grain growth. *Mater Sci Eng* 1995;**A195**:179–87.
26. Raj PM, Odulena A, Cannon WR. Anisotropic shrinkage during sintering of particles-oriented systems-numerical simulation and experimental studies. *Acta Mater* 2002;**50**:2559–70.